

The following publication Lu, H., Lyu, X., Cheng, H., Ling, Z., & Guo, H. (2019). Overview on the spatial-temporal characteristics of the ozone formation regime in China. *Environmental Science: Processes & Impacts*, 21(6), 916-929 is available at <https://doi.org/10.1039/C9EM00098D>.

1 Overview on the spatial-temporal characteristics of ozone formation regime in China

2 Haoxian Lu<sup>1</sup>, Xiaopu Lyu<sup>1</sup>, Hairong Cheng<sup>2</sup>, Zhenhao Ling<sup>3</sup>, Hai Guo<sup>1\*</sup>

3

4 1. Air Quality Studies, Department of Civil and Environmental Engineering, The Hong Kong  
5 Polytechnic University, Hong Kong, China

6 2. School of Resource and Environmental Sciences, Wuhan University, Wuhan, China

7 3. School of Atmospheric Sciences, Sun Yat-sen University, Guangzhou, China

8 \* Corresponding author. [ceguohai@polyu.edu.hk](mailto:ceguohai@polyu.edu.hk)

9

## 10 **Abstract**

11 Ozone (O<sub>3</sub>), a main component in photochemical smog, is a secondary pollutant formed  
12 through complex photochemical reactions involving nitrogen oxides (NO<sub>x</sub>) and volatile  
13 organic compounds (VOCs). Since the past decades, with the rapid economic  
14 development, industrialization and urbanization, the mixing ratio of O<sub>3</sub> has been  
15 increased substantially in China. O<sub>3</sub> non-attainment days have been frequently observed.  
16 Despite great efforts made in these years, it is still difficult to alleviate O<sub>3</sub> pollution in  
17 China, due to its non-linear relationship with the precursors. In view of the severe  
18 situation in China, this study carries out a comprehensive review on the spatial-temporal  
19 variations of relationship between O<sub>3</sub> and its precursors (i.e. O<sub>3</sub> formation regime), built  
20 upon the previous reviews of the spatial-temporal variations of O<sub>3</sub> and its precursors  
21 levels. Valuable findings from previous studies were laid out for better understanding  
22 of O<sub>3</sub> pollution, followed by implications for the control of O<sub>3</sub> pollution. Literature  
23 review indicates that O<sub>3</sub> formation in most areas of North China Plain (NCP), Yangtze  
24 River Delta (YRD) and Pearl River Delta (PRD) regions is in a VOC-limited regime  
25 during the high-O<sub>3</sub> seasons due to dramatic emissions from human activities in cities.  
26 Out of these metropolitan areas, NO<sub>x</sub>-limited regime dominates rural/remote areas.  
27 From summer to winter, O<sub>3</sub> formation regime over China shows a tendency to shift to  
28 a VOC-limited regime. Furthermore, O<sub>3</sub> formation in China moved toward increasing  
29 sensitivity to VOC emissions before the 12<sup>th</sup>-Five-Year-Plan. However, after the 12<sup>th</sup>-  
30 Five-Year-Plan, successful reduction of NO<sub>x</sub> slowed down this trend. Further effective

31 controls of VOCs are expected to achieve sustained O<sub>3</sub> attainment in the future. To  
32 timely solve the current O<sub>3</sub> pollution problem, precise control of O<sub>3</sub> precursors is  
33 proposed, together with the joint prevention and control of regional air pollution.

34 **Key words:** Ozone; O<sub>3</sub> formation regime; Spatial-temporal; China

35

## 36 **1. Introduction**

37 Because of the rapid industrialization and urbanization in China, air pollution, such as  
38 haze and photochemical smog characterized by high-levels of fine particulate matters  
39 and/or ozone (O<sub>3</sub>), has become more and more severe and aroused public attention in  
40 recent years. Due to its strong oxidative capacity, surface O<sub>3</sub> poses adverse effects on  
41 humans' health (Goodman et al., 2015; Sousa et al., 2013), growth and productivity of  
42 crops (Bhatia et al., 2012), visibility (Aneja et al., 2004) and climate change (Ogundele  
43 et al., 2011). To study O<sub>3</sub> pollution in China, nationwide O<sub>3</sub> monitoring has been  
44 systematically conducted by the China National Environmental Monitoring Center  
45 (CNEMC) and the local Environmental Monitoring Centers since 2013  
46 (<http://www.mep.gov.cn/>), and extensive field measurements were also taken from time  
47 to time by scientists over the past 20 years. Particularly, most of the measurements were  
48 undertaken in North China Plain (NCP), Yangtze River Delta (YRD) and Pearl River  
49 Delta (PRD) regions, where severe O<sub>3</sub> pollution has been often observed (Wu and Xie,  
50 2017; Wang et al., 2017a). The characteristics of tropospheric O<sub>3</sub> pollution in China are  
51 high concentrated, long lasting, wide spread, and yearly increasing. On one hand, most  
52 cities such as Beijing, Tianjin, Shanghai, Nanjing, Guangzhou and Hong Kong  
53 frequently suffered from high-level O<sub>3</sub> exposures, which exceeded either the National  
54 Ambient Air Quality Standard (maximum hourly O<sub>3</sub> of 200 µg/m<sup>3</sup> ≈ 100 ppbv) or the  
55 World Health Organization Standard (maximum daily 8-h average (MDA8) O<sub>3</sub> > 50  
56 ppbv), and sometimes were even as high as 200 ppbv (Guo et al., 2013; Han et al.,  
57 2013; He et al., 2012; Cheng et al., 2010; Tu et al., 2007; Wang et al., 2006a). In  
58 addition, a recently nationwide study found that four cities including Beijing,

59 Chengdu, Guangzhou and Shanghai suffered from O<sub>3</sub> exposure with MDA8 > 50  
60 ppbv on more than 30% of the days from 2013 to 2015 (Wang et al., 2017b).  
61 Compared to other industrialized regions in the world (i.e. Japan, South Korea, Europe  
62 and the United States), the magnitude and frequency of high-ozone events were much  
63 greater in China by analyzing the data of surface O<sub>3</sub> in 2013-2017 (Lu et al., 2018). On  
64 the other hand, it was revealed that the continuous increases of O<sub>3</sub> levels were found in  
65 China, not only in rural/remote areas but also in residential areas ( $p < 0.05$ ). In  
66 rural/remote areas, a continuous increase of surface O<sub>3</sub> was firstly observed and  
67 reported by Wang et al. (2009) in the background atmosphere of PRD, South China,  
68 from 1994 to 2007. After that, increases of surface O<sub>3</sub> were reported likewise at other  
69 rural sites in NCP and YRD in the past decade (Ma et al., 2016; Lin et al., 2009; Wang  
70 et al., 2006b). In residential areas, the nationwide O<sub>3</sub> monitoring at 617 stations in  
71 densely populated regions by CNEMC showed that the yearly average MDA8 O<sub>3</sub>  
72 increased from 76.47 ppbv in 2013 to 82.60 ppbv in 2015 (Wang et al., 2017b).  
73 Moreover, a recent nationwide study reported that the monthly mean MDA8 O<sub>3</sub> in  
74 the four megacity clusters (i.e. Beijing–Tianjin–Hebei (BTH), YRD, PRD, and  
75 Sichuan Basin (SCB)) all showed increasing trends in the summers of 2013 to 2017  
76 except for some locations in PRD (Li et al., 2019). Hence, the tropospheric O<sub>3</sub>  
77 pollution has become a critical issue in China.

78 The tropospheric O<sub>3</sub> is generally contributed by two sources, namely, the stratospheric  
79 intrusion of O<sub>3</sub> to the troposphere, and the chemical reactions involving nitrogen oxide  
80 (NO<sub>x</sub>), volatile organic compounds (VOCs) and highly reactive radicals (e.g., hydroxyl  
81 radical (OH) and hydroperoxyl radical (HO<sub>2</sub>)) in the presence of sunlight in the  
82 troposphere (Wang et al., 2017a; Steinfeld, 1998). However, the direct stratospheric O<sub>3</sub>  
83 intrusion to the troposphere is very minor and most ground-level O<sub>3</sub> is formed in the  
84 troposphere from the photochemical reactions above (Altshuller, 1984;  
85 <https://www.epa.gov/roe/>). Therefore, control focus should be on the chemical  
86 formation of O<sub>3</sub> in the troposphere. To achieve the purpose, it is essential to fully

87 understand the spatial-temporal variations of O<sub>3</sub>, its precursors (i.e. VOCs and NO<sub>x</sub>)  
88 and their relationships so as to implement appropriate control measures for the  
89 remediation of O<sub>3</sub> pollution. Though the spatial-temporal variations of O<sub>3</sub> and its  
90 precursors over China were overviewed in previous papers, as well as the detailed  
91 formation mechanisms of O<sub>3</sub> with its precursors (Diao et al., 2018; Guo et al., 2017;  
92 Wang et al., 2017a), the spatial-temporal patterns of the relationship of O<sub>3</sub> with its  
93 precursors (i.e. O<sub>3</sub> formation regime) have not been comprehensively reviewed and  
94 summarized. In fact, the non-linear relationship of O<sub>3</sub> with its precursors makes the O<sub>3</sub>  
95 pollution complicated, leading to continuous increase of O<sub>3</sub> level despite the  
96 implementation of intensive control measures in recent years. Therefore, understanding  
97 the spatial-temporal patterns of O<sub>3</sub> formation regime would help us determine the most  
98 efficient approach for O<sub>3</sub> reduction. All the studies of O<sub>3</sub> formation regime over the past  
99 20 years in China were thoroughly reviewed in this paper. To our best knowledge, this  
100 paper is in fact the first comprehensive review on the spatial-temporal characteristics  
101 of O<sub>3</sub> formation regime in China.

102 This review paper mainly focuses on the O<sub>3</sub> formation regimes in different regions in  
103 China. The 'Introduction' section provides the background and significance of the  
104 review; The Section 2 reviews the spatial variations of O<sub>3</sub> formation regimes in China;  
105 The Section 3 summarizes the seasonal, diurnal and long-term patterns of O<sub>3</sub> formation  
106 regimes in China; and the Section 4 provides some directions for the control of O<sub>3</sub>  
107 pollution.

108

## 109 **2. Spatial variations of O<sub>3</sub> formation regimes**

110 In general, O<sub>3</sub> formation regimes can be classified into three categories: VOC-limited  
111 (VOC-sensitive), NO<sub>x</sub>-limited (NO<sub>x</sub>-sensitive) and transition regime. The cause of  
112 different O<sub>3</sub> formation regimes is mainly attributed to the dual role of NO<sub>x</sub> in O<sub>3</sub>  
113 formation by regulating the chemistry of HO<sub>x</sub> radicals. On one hand, NO<sub>x</sub> drives O<sub>3</sub>  
114 formation through the photochemical cycle involving NO<sub>x</sub>, atomic oxygen (O), O<sub>2</sub> and

115 sunlight. On the other hand, NO<sub>x</sub> retards the rate of O<sub>3</sub> formation through the reactions  
116 with HO<sub>x</sub> radicals to remove OH from oxidation cycle and produce relatively non-  
117 reactive species such as HNO<sub>3</sub>. Moreover, the peroxy radicals (i.e. HO<sub>2</sub> and RO<sub>2</sub>)  
118 generated from the reactions of VOCs with OH efficiently convert NO to NO<sub>2</sub>, resulting  
119 in the accumulation of O<sub>3</sub> due to lack of NO titration effect ( $\text{NO} + \text{O}_3 \rightarrow \text{NO}_2 + \text{O}_2$ ) (Jenkin  
120 and Clemitshaw, 2000; Sillman, 1999; Barker, 1995; Wang et al., 2017a). Therefore, at  
121 low VOC/NO<sub>x</sub> conditions, the reaction between OH and NO<sub>2</sub> is the dominant chain  
122 terminating reaction, competing with chain propagating reactions of OH and VOCs.  
123 Reducing the concentration of VOCs would lead to a decrease in O<sub>3</sub> formation (VOC-  
124 limited regime). On the other hand, at high VOC/NO<sub>x</sub> ratios, reactions of OH and VOCs  
125 are the dominant chain terminating reactions, while the oxidation of NO to NO<sub>2</sub> by HO<sub>2</sub>  
126 and RO<sub>2</sub> is the key propagating reaction, which forms O<sub>3</sub> consequently. Hence, any  
127 reduction in NO<sub>x</sub> would decrease the photochemical O<sub>3</sub> formation (NO<sub>x</sub>-limited  
128 regime). Lastly, when the levels of VOCs and NO<sub>x</sub> are comparative, the reaction of OH  
129 with neither VOCs nor NO<sub>x</sub> is dominant and thus O<sub>3</sub> formation is limited by both NO<sub>x</sub>  
130 and VOCs. Namely, O<sub>3</sub> level is reduced by cutting both precursors (transition regime).  
131 To determine O<sub>3</sub> formation regimes, there were a number of methods used to investigate  
132 the O<sub>3</sub>-precursors relationship, including relative ratios of VOCs/NO<sub>x</sub>, observed  
133 indicators (i.e., O<sub>3</sub>/NO<sub>z</sub>, H<sub>2</sub>O<sub>2</sub>/NO<sub>z</sub> or H<sub>2</sub>O<sub>2</sub>/HNO<sub>3</sub>), correlation analysis of O<sub>3</sub> with  
134 VOCs and NO<sub>x</sub>, observation-based model (OBM) and emission-based model (EBM),  
135 which were comprehensively concluded and discussed by Wang et al. (2017a) and Guo  
136 et al. (2017). The first three approaches simply use the field measurement data of O<sub>3</sub>  
137 and its precursors to identify O<sub>3</sub> formation regimes. VOCs/NO<sub>x</sub> ratios reflect the  
138 abundant O<sub>3</sub> precursors at a specific site and determine the O<sub>3</sub> formation regime based  
139 on the experiential criteria in previous studies. Similarly, the values of observed  
140 indicators represent the dominant precursor and/or reaction in O<sub>3</sub> formation according  
141 to the standards summarized from previous studies and thus indicate O<sub>3</sub> formation  
142 regimes. Correlation analysis of O<sub>3</sub> with VOCs and NO<sub>x</sub> visually display the

143 relationship of O<sub>3</sub> with its precursor based on large quantities of averaged data covering  
144 multiple days. Although these approaches are simple and straightforward, they are not  
145 completely reliable by themselves and do not provide comprehensive analyses on the  
146 nonlinear O<sub>3</sub> formation mechanism. In addition to the three approaches, the sensitivity  
147 of O<sub>3</sub> production to various O<sub>3</sub> precursors can be quantified by conducting sensitivity  
148 modeling analyses with an assumed reduction in the concentration of target precursors  
149 via OBM and EBM. OBM simulates O<sub>3</sub> formation by inputting measurements of  
150 gaseous pollutants and meteorological conditions, while EBM simulates O<sub>3</sub> formation  
151 by importing the emission of VOCs and NO<sub>x</sub> from the emission inventory. Compared  
152 to EBM, OBM simulates O<sub>3</sub> photochemical production and destruction based on  
153 measured ambient concentrations of O<sub>3</sub> and its precursors, which can avoid the  
154 uncertainties caused by emission inventories and the simulated boundary layer  
155 dynamics (Russell and Dennis, 2000). Nevertheless, EBM is able to study O<sub>3</sub> pollution  
156 without the restriction of observation data and break the limitations of time and space  
157 to investigate O<sub>3</sub> formation in a large-scale region and expected time period. It is  
158 noteworthy that the determination of different O<sub>3</sub> formation regimes is difficult to reach  
159 an agreement since it is dependent on the approach used for analysis of the O<sub>3</sub>-precursor  
160 relationships, and the criteria of different approaches are not the same. Despite the  
161 potential differences of results, O<sub>3</sub> formation regime is basically determined by how the  
162 O<sub>3</sub> formation responds to the changes of its precursors, no matter which method is  
163 adopted.

164 Previous studies indicated that large amount of O<sub>3</sub> precursors was emitted in the NCP,  
165 YRD and PRD regions - the most developed regions in China, and thus led to the  
166 elevated O<sub>3</sub> levels in these regions with continuously increasing trends in these years  
167 (Diao et al., 2018; Guo et al., 2017; Wang et al., 2017a). Among the three regions, the  
168 highest maximum O<sub>3</sub> and VOCs concentrations were found in NCP, followed by PRD  
169 and YRD. In addition, all these three regions had comparable and high NO<sub>x</sub> emissions.  
170 Furthermore, the levels of O<sub>3</sub> and its precursors varied in different land-use function

171 areas in these regions. In urban/populated areas, the levels of O<sub>3</sub> precursors were usually  
172 higher due to the massive anthropogenic emissions. However, higher values of  
173 maximum hourly O<sub>3</sub> were mostly observed in rural/remote areas because of the aging  
174 of air masses. Similarly, the relationship of O<sub>3</sub> with its precursors was extensively  
175 explored in NCP, YRD and PRD regions for seeking enlightenments on O<sub>3</sub> pollution  
176 control, especially in summer and autumn, when O<sub>3</sub> levels were usually higher due to  
177 the favorable circumstances for O<sub>3</sub> formation (i.e. high temperature, strong solar  
178 radiation, low relative humidity and high precursors levels) (Wang et al., 2017a). The  
179 detailed review on the spatial variations of O<sub>3</sub> formation regime using the above  
180 approaches in the three regions during the high-O<sub>3</sub> seasons is given below.

## 181 **2.1** The NCP region

182 Different O<sub>3</sub> formation regimes were frequently found in NCP during the high-O<sub>3</sub>  
183 season (i.e. summer). Representative studies are listed in Table 1. Most of these studies  
184 in NCP were conducted in Beijing and its surrounding areas. In general, NO<sub>x</sub>-limited  
185 regimes were found in the rural/remote areas, whereas urban/populous areas were under  
186 the VOC-limited regimes. Besides, transition regime was more frequently found in  
187 NCP than in PRD and YRD.

188 VOC-limited regimes dominated in the urban areas of Beijing, a densely-populated city  
189 with serious pollution problems (Zhang et al., 2014; Tang et al., 2010; Chou et al., 2009;  
190 Shao et al., 2009a; Xu et al., 2008). By adopting different emission inventories in  
191 different domains in a community multiscale air quality (CMAQ) model, Xu et al.  
192 (2008) revealed that in summer 2000, the urban areas of Beijing were generally in a  
193 VOC-limited regime, while the urban downwind areas changed gradually to a NO<sub>x</sub>-  
194 limited condition. Similarly, sensitivity analysis of O<sub>3</sub> formation in central urban  
195 Beijing was performed by Tang et al. (2010) in August 2006 using the Nested Air  
196 Quality Prediction Model System (NAQPMS). It was found that abatement of the most  
197 contributing VOCs could be more efficient on reducing the high levels of surface O<sub>3</sub>,  
198 while inadequate abatement of NO<sub>x</sub> would lead to a reverse outcome. Apart from model

199 simulation, a few field measurements at PKU (an urban site) in summer proved that O<sub>3</sub>  
200 formation was mostly in a VOC-limited regime (Zhang et al., 2014; Chou et al., 2009;  
201 Shao et al., 2009a). In addition to Beijing, a VOC-limited regime was also identified at  
202 an urban site in Tianjin (i.e. Tieta) using the NCAR-Master Mechanism model (NCAR-  
203 MM) to reveal the response of local O<sub>3</sub> to the emissions of its precursors during July-  
204 August of 2010 and 2011 (Wei et al., 2015).

205 Furthermore, NO<sub>x</sub>-limited regime in NCP was reported by few studies. A 5-week field  
206 campaign was conducted at a suburban site in Tianjin in summer 2009. In the study, a  
207 NO<sub>x</sub>-limited regime was identified, diagnosed by the VOCs/NO<sub>x</sub> ratios and further  
208 verified by a photochemical box model (i.e. NCAR-MM) (Ran et al., 2011). Apart from  
209 field measurements, the chemical sensitivity of O<sub>3</sub> formation over NCP region was  
210 investigated in summer 2015 by a recent study using the regional atmospheric modeling  
211 system-community multiscale air quality (RAMS-CMAQ) (Han et al., 2018). Results  
212 indicated that NO<sub>x</sub>-sensitive regimes dominated in remote/rural areas in the NCP.

213 Besides, areas in NCP were frequently found under transition regimes. For instance,  
214 from a sampling campaign at PKU and Yufa (a rural site) in summer 2006, transition  
215 regimes were identified at both sites by two studies (Lu et al., 2010; Shao et al., 2009a).

216 On one hand, Lu et al. (2010) adopted the relative incremental reactivity (RIR) values  
217 and the parameter  $L_N/Q$  (fraction of radicals removed by reaction with NO<sub>x</sub> related to  
218 total radical production rates) to determine the O<sub>3</sub> formation regime. It was reported  
219 that NO<sub>x</sub>-sensitive and VOC-sensitive regimes existed and frequently shifted to each  
220 other at both sites. On the other hand, Shao et al. (2009a) analyzed the O<sub>3</sub> formation  
221 regime at Yufa through the correlation between the daily maximum O<sub>3</sub> and the initial  
222 VOCs and NO<sub>x</sub> level (correlation:  $[O_3]_{\max} = 0.26[VOCs]_{\text{initial}} + 2.24[NO_x]_{\text{initial}} + 48.9$ ).

223 The correlation suggested that O<sub>3</sub> formation was sensitive to both emissions of VOCs  
224 and NO<sub>x</sub>. Moreover, a recent study at a rural site downwind of Jinan in summer 2013  
225 suggested that O<sub>3</sub> production was in a transition regime, analyzed by the OBM model  
226 (Zong et al., 2018). In addition to measurement-based analyses, Liu et al. (2012)



227 simulated the summertime photochemistry near the surface in Beijing in 2007 using a  
 228 1-D photochemical model. It was found that O<sub>3</sub> production was neither NO<sub>x</sub>-limited  
 229 nor VOC-limited, but was in a transition regime. Furthermore, a recent model study  
 230 indicated that the emissions of VOCs and NO<sub>x</sub> both vastly influenced O<sub>3</sub> formation in  
 231 the suburban areas of NCP region in summer 2015 (Han et al., 2018).

232

233 **Table 1 Summary of the studies of O<sub>3</sub> formation regime in the NCP**

City	Site/Area	Year & Season	Land-use function	O <sub>3</sub> formation regime	Method	Reference
<b>Beijing</b>	PKU	2004-2006, Summer	Urban	VOC-limited	Correlation analysis	Shao et al. (2009a)
		2005-2011, Summer	Urban	VOC-limited	Observation-based model & Correlation analysis	Zhang et al. (2014)
		2006, Summer	Urban	VOC-limited	Observation-based model	Chou et al. (2009)
		2007, Summer	Urban	Transition	Emission-based model	Liu et al. (2012)
		2006, Summer	Urban	Transition	Observation-based model	Lu et al. (2010)
	Yu Fa		Rural			
		2004-2006, Summer	Rural		Correlation analysis	Shao et al. (2009a)
	Central urban Beijing	2006, Summer	Urban	VOC-limited	Emission-based model	Tang et al. (2010)
<b>The whole Beijing</b>	N/A	2000, Summer	Urban	VOC-limited	Emission-based model	Xu et al. (2008)
			Urban downwind area	NO <sub>x</sub> -limited		
<b>Tianjin</b>	Wu Qing	2009, Summer	Suburban	NO <sub>x</sub> -limited	Observation-based model	Ran et al. (2011)
	Tieta	2010-2011, Summer	Urban	VOC-limited	Observation-based model	Wei et al. (2015)
<b>Jinan</b>	Yu Cheng	2013, Summer	Rural	Transition	Observation-based model	Zong et al. (2018)
<b>The whole NCP</b>	N/A	2015, Summer	Rural	NO <sub>x</sub> -limited	Emission-based model	Han et al. (2018)
			Sub-urban	Transition		

234

## 235 **2.2 The YRD region**

236 Compared to PRD and NCP, fewer studies were carried out in YRD. Nevertheless,  
 237 cities/areas under different O<sub>3</sub> formation regimes (i.e. VOC-limited and NO<sub>x</sub>-limited  
 238 regime) were still reported by a few studies, which are summarized in Table 2. Briefly,  
 239 O<sub>3</sub> formation in most of the areas in YRD was under VOC-limited regimes. Shanghai  
 240 and Nanjing were the two popular cities for investigating the O<sub>3</sub> formation regime.

241 Previous studies indicated that Shanghai and its surrounding cities were basically in  
 242 VOC-limited regimes (Xu et al., 2017; An et al., 2015; Xue et al., 2014; Tang et al.,  
 243 2008; Geng et al., 2008). For instance, it was reported that O<sub>3</sub> production at two urban  
 244 sites in Shanghai was situated in a non-methane organic compounds (NMOC)-limited  
 245 regime based on the ratios of VOCs/NO<sub>x</sub> (Ran et al., 2009; Tang et al., 2008). Consistent  
 246 result was found by Li et al. (2012a) in urban Shanghai with the help of a CMAQ  
 247 modeling system with Carbon Bond 05 (CB05) chemical mechanism. Aside from urban  
 248 areas, a VOC-limited regime was also identified at a suburban site near Shanghai in  
 249 summer 2005 using a photochemical box model with master chemical mechanism  
 250 (PBM-MCM) (Xue et al., 2014). In addition to Shanghai, VOC-sensitive regimes  
 251 existed likewise in Nanjing. For instance, by analyzing the VOCs/NO<sub>x</sub> ratios and RIR  
 252 values, An et al. (2015) proved that the O<sub>3</sub> formation in Pancheng town (a rural site)  
 253 was VOC-limited in the summer of 2013. Moreover, the same O<sub>3</sub> formation regime was  
 254 found at the station for Observation Regional Processes of the Earth System (SORPES)  
 255 in Nanjing (a suburban site) by two studies. One was analyzed through the OBM  
 256 method based on the data collected on National Day holiday in 2014 (Xu et al., 2017)  
 257 and the other was indicated by the correlations of CO-NO<sub>y</sub>-O<sub>3</sub> using the data collected  
 258 in 2011 for one year (Ding et al., 2013).  
 259 Moreover, NO<sub>x</sub>-sensitive regime and transition regime were barely found in YRD based  
 260 on observation-based studies. Nevertheless, with the help of a CMAQ modeling system  
 261 with Carbon Bond 05 (CB05) chemical mechanism, Li et al. (2012a) pointed out that  
 262 NO<sub>x</sub>-sensitive regime existed in rural areas of YRD in summer 2010, such as Jinshan  
 263 district in Shanghai.

264 Table 2 Summary of the studies of O<sub>3</sub> formation regime in the YRD

City	Site/Area	Year & Season	Land-use function	O <sub>3</sub> formation regime	Method	Reference
Shanghai	Tai Cang	2005, Summer	Suburban	VOC-limited	Observation-based model	Xue et al. (2014)
	Song Jiang	2006-2007, All seasons	Urban	VOC-limited	VOCs/ NO <sub>x</sub> ratios	Ran et al. (2009)
	Xu Jia Hui	2006, Summer to Winter	Urban	VOC-limited	VOCs/ NO <sub>x</sub> ratios	Tang et al. (2008)

<b>Nanjing</b>	Pan Cheng	2013, Summer	Suburban	VOC-limited	Observation-based model	An et al. (2015)
	The Station for Observing Regional Processes of the Earth system	2011, Summer	Rural	VOC-limited	Correlation analysis	Ding et al. (2013)
	Xian Lin	2014, Summer (National Day holidays)	Suburban	VOC-limited	Observation-based model	Xu et al. (2017)
<b>Urban Shanghai</b>	N/A	2010, Summer	Urban	VOC-limited	Emission-based model	Li et al. (2012a)
<b>Suburban Shanghai (Jinshan)</b>			Suburban	NO <sub>x</sub> -limited		
<b>Nanjing</b>			Urban	N/A		
<b>Hangzhou</b>			Urban	N/A		

### 265 2.3 The PRD region

266 Numerous studies have investigated the O<sub>3</sub> formation regime in PRD during the high-  
267 O<sub>3</sub> seasons (i.e. summer and autumn) over the past 20 years, especially in Hong Kong  
268 and the inland PRD region. Summary of these studies is shown in Table 3. Basically,  
269 O<sub>3</sub> formation was controlled by the emission of VOCs in most of the areas of PRD,  
270 which was consistent with the result of previous studies (Wang et al., 2017a; Guo et al.,  
271 2017), whereas the other O<sub>3</sub> formation regimes (i.e. NO<sub>x</sub>-limited and transition regime)  
272 were only found out of the densely populated areas/cities.

273 Different approaches used in previous studies have proved that most of the areas in  
274 PRD were under VOC-limited regimes. In 2000, gaseous pollutants and VOCs samplers  
275 were measured in the central of Guangzhou from summer to autumn. It was reported  
276 that O<sub>3</sub> formation was generally limited by the concentrations of VOCs according to  
277 the RIR values extracted from the OBM model (Shao et al., 2009b). In addition to urban  
278 areas, several studies pointed out that VOC-limited regimes also existed in rural areas  
279 of Guangzhou (Xue et al., 2014; Cheng et al., 2010; Zhang et al., 2008). Apart from  
280 Guangzhou, areas under VOC-sensitive regimes were found in Hong Kong as well.  
281 From 23 October to 01 December 2007, ambient O<sub>3</sub> and its precursors were measured  
282 at Tung Chung (TC), a suburban site in Hong Kong. Using the database, two studies  
283 reported that O<sub>3</sub> production at TC was generally VOC-limited, which meant reducing  
284 VOCs decreased the O<sub>3</sub> formation and reducing NO<sub>x</sub> could increase O<sub>3</sub> level (Cheng et  
285 al., 2010; Guo et al., 2009). Moreover, from 6 September to 29 November 2010, a field

286 measurement of O<sub>3</sub> and its precursors was conducted at Tai Mo Shan (TMS) and Tsuen  
287 Wan (TW) (a rural site and an urban site, respectively). The O<sub>3</sub> formation regimes at  
288 two sites were revealed. At TMS, photochemical O<sub>3</sub> formation was mostly influenced  
289 by VOCs with a measurable effect of NO<sub>x</sub> according to the RIR analysis (Guo et al.,  
290 2013), while O<sub>3</sub> concentration was negatively correlated with NO<sub>x</sub> at TW, implying that  
291 O<sub>3</sub> formation was primarily VOC-sensitive, further validated by the VOCs/NO<sub>x</sub> ratios  
292 and RIR values (Ling and Guo, 2014; Lam et al., 2013). Aside from measurement-based  
293 analyses, consistent results were obtained using the emission-based models. By using  
294 a WRF/SMOKE-PRD/CMAQ modeling system to explore the photochemistry over the  
295 entire PRD region in August and October 2010, Ou et al. (2016) suggested that intensive  
296 controls of anthropogenic VOC were more efficient for short-term despike of peak  
297 O<sub>3</sub> levels in urban and port areas of PRD. The results were in line with another modeling  
298 study, which reported that O<sub>3</sub> formation was VOC-limited in the central inland PRD,  
299 PRE, and surrounding coastal areas in autumn 2004 (Wang et al., 2010). In addition, a  
300 modeling study investigated the peculiarity of O<sub>3</sub> episode days in Hong Kong in  
301 summer 2005 by a high-resolution air quality model (Pollutants in the Atmosphere and  
302 Their Transport in Hong Kong (PATH)). It was pointed out that the chemical regime for  
303 O<sub>3</sub> formation in Hong Kong seemed to be mainly limited by VOCs (Huang et al., 2005).  
304 Furthermore, NO<sub>x</sub>-limited regime was only found in rural areas of PRD by few  
305 modeling studies. Based on the anthropogenic emissions inventory and the biogenic  
306 emissions inventory provided by HKEPD and inland PRD authority, Wang et al. (2010)  
307 simulated O<sub>3</sub> pollution over the PRD region in October 2004. Results showed that O<sub>3</sub>  
308 formation was generally NO<sub>x</sub>-limited in rural southwestern PRD, where the air masses  
309 were photochemically aged. Moreover, Ou et al. (2016) indicated that O<sub>3</sub> formation was  
310 always NO<sub>x</sub>-limited at a rural site in PRD (Jiangmen) on the O<sub>3</sub> episode days in August,  
311 based on the O<sub>3</sub> isopleth profiles obtained from a WRF/SMOKE-PRD/CMAQ  
312 modeling system.

313 Noteworthy, shift among different O<sub>3</sub> formation regimes was reported by few field

314 studies in PRD, which indicated that O<sub>3</sub> formation was limited by both VOCs and NO<sub>x</sub>.  
 315 For instance, the chemical sensitivity of O<sub>3</sub> formation was investigated at a remote  
 316 island site (Wan Shan Island) in 2013. Results found that O<sub>3</sub> production at the oceanic  
 317 site changed from transition regimes on non-O<sub>3</sub> episode days to VOC-limited regimes  
 318 on O<sub>3</sub> episode days (Wang et al., 2018). Moreover, at a suburban site in Guangzhou (i.e.  
 319 Panyu), O<sub>3</sub> formation in summer and autumn was usually NO<sub>x</sub>-limited at noon but  
 320 shifted to VOC-limited when O<sub>3</sub> concentrations became low in the morning and at night  
 321 according to the VOC/NO<sub>x</sub> ratios (Zou et al., 2015). In addition to field studies,  
 322 transition regimes were also identified at a suburban site and a rural site in Guangdong  
 323 in the summer and autumn of 2010, respectively, with the help of the WRF/SMOKE-  
 324 PRD/CMAQ modeling system (Ou et al., 2016).

325  
326

Table 3 Summary of the studies of O<sub>3</sub> formation regime in the PRD

City	Site/Area	Year & Season	Land-use function	O <sub>3</sub> formation regime	Method	Reference
<b>Guangzhou</b>	Guangzhou Research Institute of Environmental Protection	2000, Summer -Autumn	Urban	VOC-limited	Observation-based model	Shao et al. (2009b)
	Wan Qin Sha	2007, Autumn to Winter	Rural	VOC-limited	Observation-based model	Cheng et al. (2010)
		2004, Summer		VOC-limited	Observation-based model	Xue et al. (2014)
	Xin Ken	2004, Autumn	Rural	VOC-limited	Observation-based model	Zhang et al. (2008)
	Pan Yu	2011-2012, Summer & Autumn	Suburban	Transition	VOC/NO <sub>x</sub> ratios	Zou et al. (2015)
<b>Hong Kong</b>	Tsuen Wan	2010, Summer to Autumn	Urban	VOC-limited	Observation-based model	Ling and Guo (2014), Lam et al. (2013)
	Tai Mo Shan		Rural	VOC-limited	Observation-based model	Guo et al. (2013)
	Wan Shan Island	2013, Summer to Autumn	Rural	Transition	Observation-based model	Wang et al. (2018)
	Tung Chung	2007, Autumn to Winter	Suburban	VOC-limited	Observation-based model	Cheng et al. (2010), Guo et al. (2009)
<b>The whole Hong Kong</b>	N/A	2004, Summer	N/A	VOC-limited	Emission-based model	Huang et al. (2005)
<b>Guangzhou</b>	N/A	2010, Summer	Urban	VOC-limited	Emission-based model	Ou et al. (2016)
		Autumn				
<b>Dongguan</b>		2010, Summer	Suburban	Transition		
		Autumn		VOC-limited		

<b>Nansha</b>		2010, Summer Autumn	Suburban	VOC-limited		
<b>Jiangmen</b>		2010, Summer Autumn	Rural	NO <sub>x</sub> -limited Transition		
<b>The whole PRD</b>	The central inland PRD and coastal area	2004, Autumn	Urban/Suburban	VOC-limited	Emission-based model	Wang et al. (2010)
	The rural southwestern PRD		Rural	NO <sub>x</sub> -limited		

327

## 328 2.4 Other regions

329 Apart from the three most developed regions above, the O<sub>3</sub> formation regimes were  
330 also investigated in cities of other regions, as shown in Table 4. In Lanzhou, O<sub>3</sub> was  
331 formed under a NO<sub>x</sub>-sensitive regime at a suburban site while VOC-sensitive regime  
332 was found in downtown area in summer 2013 according to the O<sub>3</sub>-isopleth plots (Jia et  
333 al., 2016). The result was consistent with the previous study of Xue et al. (2014), which  
334 conducted a field measurement at other rural site in Lanzhou in 2006. Moreover, in  
335 Wuhan, the central China, O<sub>3</sub> formation was mostly controlled by the emission of VOCs  
336 (except July 2013) because of the great contribution of vehicle emission and coal  
337 burning (Lyu et al., 2016). In southwestern China, Tan et al. (2018) investigated the O<sub>3</sub>  
338 formation regime at four sites in Chengdu using an OBM model and found that  
339 reduction of anthropogenic VOCs was the most efficient way to mitigate O<sub>3</sub> pollution  
340 since most of the sampling sites were under the VOC-limited regimes. At this stage,  
341 summary of O<sub>3</sub> formation regime in other regions besides NCP, YRD and PRD is  
342 difficult to achieve due to the limited references. More intensive studies are expected  
343 to fill the knowledge gap in the future.

344 Table 4 Summary of the studies of O<sub>3</sub> formation regime in other regions

City	Site/Area	Year & Season	Land-use function	O <sub>3</sub> formation regime	Method	Reference
Lanzhou	Lanzhou Environmental Monitoring Station	2013, Summer	Urban	VOC-limited	Correlation analysis	Jia et al. (2016)
	West suburban site		Suburban	NO <sub>x</sub> -limited		
	Renshoushan Park	2006, Summer	Suburban	NO <sub>x</sub> -limited	Observation-based model	Xue et al. (2014)

Wuhan	Hubei Provincial Environmental Monitoring Center	2013-2014, All seasons	Urban	VOC-limited	Observation-based model	<a href="#">Lyu et al. (2016)</a>
Chengdu	Peng Zhou Pi Xian Shuang Liu Cheng Zhong	2016, Autumn	Suburban   Urban	Transition VOC-limited	Observation-based model	<a href="#">Tan et al. (2018)</a>

345

346 Overall, O<sub>3</sub> formation in the most areas of NCP, YRD, and PRD regions is likely in a  
347 VOC-limited regime due to the vastly anthropogenic emissions of air pollutants. Out of  
348 these metropolitan areas, O<sub>3</sub> formation in rural/remote areas is mainly limited by NO<sub>x</sub>  
349 levels. Such discrepancy of O<sub>3</sub> formation regime is mainly attributed to the disparity of  
350 different O<sub>3</sub> precursors' levels in different land-use function areas. In general, NO<sub>x</sub>  
351 levels are high in metropolitan areas due to the vast emission of NO<sub>x</sub> from human  
352 activities (i.e. combustion and vehicle emission), and thus NO<sub>x</sub> is saturated for O<sub>3</sub>  
353 formation. However, NO<sub>x</sub>-limited regime dominates rural areas as VOCs are usually  
354 sufficient for O<sub>3</sub> formation because of the abundance of biological VOCs emission from  
355 plants and rare NO<sub>x</sub> emission from human activities. Furthermore, more intensive  
356 studies in other regions besides NCP, YRD and PRD are expected in the future.

357

### 358 **3. Diurnal, seasonal and long-term patterns of O<sub>3</sub> formation regimes**

359 Apart from the spatial distribution, it is pointed out that O<sub>3</sub> formation regimes in China  
360 have several temporal characteristics, including diurnal, seasonal and long-term  
361 variations ([Wu et al., 2018](#); [Jin and Holloway, 2015](#); [Brown and Stutz, 2012](#); [Liu et al.,](#)  
362 [2010](#)).

#### 363 **3.1 Diurnal variation of O<sub>3</sub> formation regimes**

364 O<sub>3</sub> pollution basically occurs in the daytime since sunlight is the major driving force  
365 for the photochemical chemistry. Therefore, majority of researches conducted O<sub>3</sub>  
366 pollution investigation during daytime. It was not until 10 years ago, night-time  
367 chemistry in the troposphere began to be explored and thus the relationships between

368 O<sub>3</sub> and its precursors at night were revealed (Brown and Stutz, 2012). Generally, O<sub>3</sub>  
369 level rises in the morning, peaks in the afternoon and then gradually declines at night  
370 (Reddy et al., 2011; Xu et al., 2008). The increase of O<sub>3</sub> in daytime is caused by the O<sub>3</sub>  
371 production sequence in the presence of sunlight, while O<sub>3</sub> concentration declines at  
372 nighttime through the process of NO<sub>x</sub> titration. In the night-time process of NO<sub>x</sub>  
373 titration, O<sub>3</sub> is firstly removed by its reaction with NO, which generates NO<sub>2</sub> and O<sub>2</sub>.  
374 This reaction also exists in the daytime. However, in the absence of the photolysis of  
375 NO<sub>2</sub> to prompt O<sub>3</sub> formation at night, the result is net conversion of O<sub>3</sub> to NO<sub>2</sub>. After  
376 that, the nitrate radical, NO<sub>3</sub>, is generated through the reaction of NO<sub>2</sub> with O<sub>3</sub>, which  
377 further consumes O<sub>3</sub> and thus reduces O<sub>3</sub> level. Detailed mechanism of night-time  
378 chemistry was summarized by a recent paper (Brown and Stutz, 2012). Overall, the O<sub>3</sub>  
379 concentration at night is mainly controlled by the NO<sub>x</sub> level.

380 Because of the typical O<sub>3</sub>-precursor relationship at night, hourly O<sub>3</sub> levels show  
381 different diurnal patterns in areas of different land-use function (e.g. urban and rural  
382 areas). Generally, O<sub>3</sub> concentrations peak at around 14:00 and decrease significantly at  
383 night in urban areas, while the peak values of O<sub>3</sub> usually appear several hours later and  
384 do not drop instantaneously after sunset in rural/remote areas due to the lower emissions  
385 of NO<sub>x</sub> from human activities. For instance, according to a field measurement of O<sub>3</sub> at  
386 an urban site and a downwind rural site around Beijing from June 2005 to September  
387 2006, 90% of the O<sub>3</sub>-episode events (hourly O<sub>3</sub> level exceeded the China's norm) took  
388 place before 16:00 at the urban site, while more than 82% of those happened at night at  
389 the rural site (Ma et al., 2011). Moreover, from another four-year measurements of O<sub>3</sub>  
390 and its precursors from 2005 to 2008 at an urban and a rural site in Beijing, peak O<sub>3</sub>  
391 value appearing time in the rural area was delayed by 2-3 hours from the time in the  
392 urban area (i.e. 14:00) (Xu et al., 2011). In addition to field measurements, Li et al.  
393 (2012a) adopted the CMAQ model to simulate the O<sub>3</sub> levels over the YRD region  
394 during the O<sub>3</sub> episode days in summer 2010. The O<sub>3</sub> concentration decreased rapidly  
395 after sunset in urban areas due to the strong effect of NO titration, whereas O<sub>3</sub> could



396 still spread to rural areas and maintain high levels. Thus, O<sub>3</sub> pollution could be a notable  
397 problem in rural areas at night.

### 398 **3.2 Seasonal variation of O<sub>3</sub> formation regimes**

399 Previous review has revealed the seasonality of O<sub>3</sub> levels in the three regions ([Wang et al., 2017a](#)). In NCP and YRD, higher O<sub>3</sub> level was generally observed in the  
400 summertime. In PRD, O<sub>3</sub> levels were high in summer and autumn but it generally  
401 reached maximum value in autumn. Though the seasonality of O<sub>3</sub> level had been clearly  
402 discussed and summarized previously, the seasonal variation of O<sub>3</sub> formation regime  
403 was still unknown. A few field measurements were conducted in different seasons to  
404 solve the puzzle previously. Based on the observation-based studies, it seemed that in  
405 urban and rural/remote areas, O<sub>3</sub> formation regime was consistent throughout the entire  
406 year, whereas it became variable in suburban area in different seasons. For example,  
407 based on the diurnal variations of O<sub>3</sub> and NO<sub>x</sub> measured in central and rural areas of  
408 Guangzhou from 2006 to 2007, the O<sub>3</sub> production in central Guangzhou was mostly  
409 VOC-limited throughout the entire year, while O<sub>3</sub> production was limited by NO<sub>x</sub> in the  
410 rural area all the time ([Zheng et al., 2010](#)). Furthermore, in downtown Shanghai (i.e.  
411 Xujiahui), [Geng et al. \(2008\)](#) reported that O<sub>3</sub> formation was mainly limited by VOCs  
412 concentrations in both summer and winter, according to the ratios of CH<sub>2</sub>O/NO<sub>y</sub> and  
413 the results of NCAR-MM model. In addition, after measuring O<sub>3</sub> and its precursors in  
414 the center of Tianjin for one year, [Liu et al. \(2016\)](#) pointed out that the central Tianjin  
415 belonged to the VOC-limited region during most seasons in view of the ratios of  
416 VOC/NO<sub>x</sub>. In contrast, at a suburban site in Guangzhou (i.e. Panyu), O<sub>3</sub> formation was  
417 more likely to be VOC-limited in spring and winter while in summer and autumn, NO<sub>x</sub>-  
418 limited regimes and VOC-limited regimes frequently shifted to each other in a day ([Zou et al., 2015](#)).

421 However, due to the limits of resource and technique, site measurements are often  
422 limited in time period and spatial extent ([Jin and Holloway, 2015](#); [Zhang et al., 2008](#)).

423 To clearly explore the season pattern of O<sub>3</sub> formation regime over China, a few recent

424 studies have employed different kinds of indicators (i.e.  $P_{\text{HNO}_3}/P_{\text{H}_2\text{O}_2}$ ,  $\text{H}_2\text{O}_2/(\text{O}_3+\text{NO}_2)$ ,  
425  $\text{O}_3/\text{NO}_x$ ,  $\text{O}_3/\text{NO}_y$ ,  $\text{HCHO}/\text{NO}_y$  and  $\text{HCHO}/\text{NO}_2$ ) to identify and analyze the sensitivity  
426 of  $\text{O}_3$  formation to VOCs and  $\text{NO}_x$  in different seasons over China (Jin and Holloway,  
427 2015; Liu et al., 2010). These photochemical indicators were proposed and developed  
428 by Sillman (1995), and were applied in previous studies (Zhang et al., 2009; Tonnesen  
429 and Dennis, 2000). By comparing and validating the values of diverse indicators in  
430 different months over China, Liu et al. (2010) proved that several megacities such as  
431 Beijing, Shanghai, Tianjin, and some big cities in the YRD and PRD regions were  
432 always under the VOC-limited conditions throughout the entire year due to large  
433 amounts of traffic and industrial emissions of  $\text{NO}_x$ . Except these metropolitan areas,  $\text{O}_3$   
434 formation over almost the entire China during summer was in a  $\text{NO}_x$ -limited regime.  
435 However, in winter, the  $\text{O}_3$  formation regime basically shifted to VOC-limited  
436 chemistry over the eastern China, as well as some major cities in most of the provinces.  
437 Furthermore, by analyzing the ratios of  $\text{HCHO}/\text{NO}_2$  (FNR ratio) over the three most  
438 developed regions (NCP, YRD, and PRD) and their surrounding areas, Jin and  
439 Holloway (2015) indicated that in high-temperature seasons (defined as near-surface  
440 air temperatures  $>20$  °C in the early afternoon), VOC-limited regimes basically  
441 dominated in the megacities (i.e. Beijing, Guangzhou and Shanghai) and cities with  
442 high density of power plants (i.e. Tangshan, Shijiazhuang and Zibo), while a widespread  
443 transitional regime was found in NCP, YRD and PRD, and  $\text{NO}_x$ -limited regime was  
444 dominant out of these regions. Similarly,  $\text{O}_3$  formation regimes in the three regions were  
445 all intended to shift to VOC-limited in winter according to the lower FNR ratios. In  
446 addition to the usage of photochemical indicators, such a shift was also discovered by  
447 Ou et al. (2016), using a WRF/SMOKE-PRD/CMAQ modeling system to investigate  
448 the seasonal differences of  $\text{O}_3$  formation regimes in the urban and port areas of PRD.

### 449 3.3 Long-term variation of $\text{O}_3$ formation regimes

450 The elevated  $\text{O}_3$  levels in China are mainly attributed to the great emission of  
451 anthropogenic pollutants in the process of industrialization and urbanization over the

452 last 20 years. After the awareness of severe O<sub>3</sub> pollution in China, dramatic controls of  
453 the emissions of VOCs and NO<sub>x</sub> were implemented by the central government,  
454 especially in the past decade. Previous studies have revealed the long-term variations  
455 of the VOCs and NO<sub>x</sub> levels before and after the implementation of control measures  
456 (Diao et al., 2018; Wang et al., 2017a). Dramatic control of industrial NO<sub>x</sub> was  
457 implemented during the China's 12<sup>th</sup>-Five-Year-Plan in 2011. Since then, the total  
458 emissions of NO<sub>x</sub> reached its peak since it had increased in 1980s and began to decline.  
459 However, compared with the successful control of NO<sub>x</sub>, the reduction of VOCs  
460 emission was delayed. No turning point of the emission of VOCs was observed up to  
461 2014 since it had also increased in 1980s. Due to the variations of O<sub>3</sub> precursors' levels,  
462 the sensitivity of O<sub>3</sub> formation to VOCs and NO<sub>x</sub> in China varied over the past decades  
463 as well.

464 Although the sensitivity of O<sub>3</sub> formation to VOCs and NO<sub>x</sub> was investigated through  
465 numerous emission-based and/or observation-based studies over the last 20 years, it is  
466 still difficult to comprehensively reveal the long-term variation of O<sub>3</sub> formation regime  
467 over China. Emission-based studies basically depend on emission inventories,  
468 meteorological inputs, chemical processes, and boundary layer dynamics, all of which  
469 have associated uncertainties, while long-term and large-scale field measurements are  
470 very rare in China. Therefore, the photochemical indicators are very suited to analyze  
471 the long-term variation of O<sub>3</sub> formation regime over China. A mass of continuous and  
472 long-term data can be obtained from the satellite in given area and time period. For  
473 example, using the satellite data of HCHO and NO<sub>2</sub> measured by NASA from 2005 to  
474 2013, Jin and Holloway (2015) revealed the variations of HCHO and NO<sub>2</sub> levels over  
475 China, and investigated the spatial-temporal variation of O<sub>3</sub> formation regime by  
476 calculating the FNR ratios. A significant increasing trend in NO<sub>2</sub> and an insignificant  
477 tendency in HCHO were observed in the three most developed regions (i.e. NCP, YRD  
478 and PRD), resulting in a widespread decrease in FNR ratios. As such, the O<sub>3</sub>  
479 photochemistry in China became more sensitive to VOCs, embodied in the spatial

480 expansion of VOC-limited and transitional regimes and the longer duration of transition  
481 and VOC-limited regimes in a year. Moreover, the study pointed out that a VOC-limited  
482 regime is likely to occur throughout eastern China as early as 2025, if no significant  
483 change in the emissions of VOCs and NO<sub>x</sub> occurs and stable trends in FNR ratios  
484 remain in the future. However, it should be noticed that the result of linear extrapolation  
485 is not reliable to be regarded as prediction since the industry and environment policies  
486 change rapidly in China. As mentioned, successful reduction of NO<sub>x</sub> has been achieved  
487 since the implementation of a series of policies in the 12<sup>th</sup> Five-Year-Plan. The ambient  
488 concentration of NO<sub>x</sub> decreased by 10.1% from 2013 to 2016 monitored from 74 mega-  
489 cities in China (Zhu et al., 2017). However, the actions on reduction of VOCs were  
490 delayed. Therefore, the shift to VOC-limited regimes will be slowed down or even some  
491 regions will change to NO<sub>x</sub>-limited regimes (Wang et al., 2017a). The assumption was  
492 supported by Wu et al. (2018), using the Ozone Monitoring Instrument (OMI) satellite  
493 remote sensing data from NASA to analyze the O<sub>3</sub> formation regime in Beijing-Tianjin-  
494 Hebei (BTH) region from 2005 to 2016. Wu et al. (2018) demonstrated that the domain  
495 of NO<sub>x</sub>-limited regime in BTH region showed a trend of increase, mainly due to the  
496 effective control of NO<sub>x</sub> emission during 12<sup>th</sup> Five-Year-Plan.

497 To sum up, literature review revealed that O<sub>3</sub> level at night was mainly controlled by  
498 the amount of NO<sub>x</sub> at a specific site. Since NO<sub>x</sub> levels are usually low in rural areas due  
499 to lack of human activities, O<sub>3</sub> pollution could be a notable problem in rural areas at  
500 night. Except the metropolitan areas, which were dominated by VOC-limited regimes  
501 throughout the entire year due to large amounts of traffic and industrial emissions of  
502 NO<sub>x</sub>, most of the areas of China intended to shift from other O<sub>3</sub> formation regimes  
503 (transition or NO<sub>x</sub>-limited regimes) in summer to a VOC-limited regime in winter. In  
504 addition, because of the dramatic increase of NO<sub>x</sub> since the 1980s, O<sub>3</sub> formation in  
505 China moved toward increasing sensitivity to VOC emissions. However, it is likely that  
506 the shift will be slowed down or even some regions will change to NO<sub>x</sub>-limited regimes  
507 owing to the delayed actions on VOCs controls and the successful reduction on NO<sub>x</sub>

508 emission during the 12<sup>th</sup>-Five-Year-Plan. Hence, effective control measures of VOCs  
509 emissions are supposed to be implemented in time.

510 In addition to variations of O<sub>3</sub> precursors' levels, changes in meteorological conditions  
511 also influence the nonlinear O<sub>3</sub> formation chemistry. [Pusede et al. \(2015\)](#)  
512 comprehensively investigated the relationship between temperature and the recent  
513 trends of the surface O<sub>3</sub> in America and proved that the chemical terms driving produces  
514 O<sub>3</sub> (PO<sub>3</sub>) vary nonlinearly with temperature. Temperature affected the PO<sub>3</sub> through  
515 influencing the reaction rates in photochemical reactions and levels of key components  
516 in O<sub>3</sub> formation (i.e. VOCs, NO<sub>x</sub> and highly reactive radicals). In a day, the reactivity  
517 of HO<sub>x</sub> radicals increases when the solar radiation and temperature go up at noon, which  
518 leads to the rapid consumption of NO<sub>x</sub> and thus the O<sub>3</sub> formation regime becomes more  
519 NO<sub>x</sub>-limited. In a year, depressed temperature and solar radiation in winter slow down  
520 the consumption of NO<sub>x</sub> through the subdued reactions with HO<sub>x</sub> radicals and thus NO<sub>x</sub>  
521 level increases and the O<sub>3</sub> formation regime shifts to a more VOC-limited regime. In  
522 decades, under the circumstance that global temperatures are projected to rise, the  
523 lifetime of NO<sub>x</sub> and peroxy nitrates (RO<sub>2</sub>NO<sub>2</sub>) decreases. NO<sub>x</sub> levels in remote areas  
524 may become lower as a result of less transportation of NO<sub>x</sub> from urban areas, while the  
525 abundance of NO<sub>x</sub> may increase in populated cities due to the stronger decomposition  
526 of RO<sub>2</sub>NO<sub>2</sub> to NO<sub>x</sub>. As such, O<sub>3</sub> formation regimes may become more VOC-limited in  
527 urban areas and more NO<sub>x</sub>-limited in remote areas driven by climate change. Overall,  
528 changes in meteorological conditions along with future changes in O<sub>3</sub> precursor  
529 emissions will alter PO<sub>3</sub> in ways that are predictable but complex.

530

#### 531 **4. Implications for the control of O<sub>3</sub> pollution**

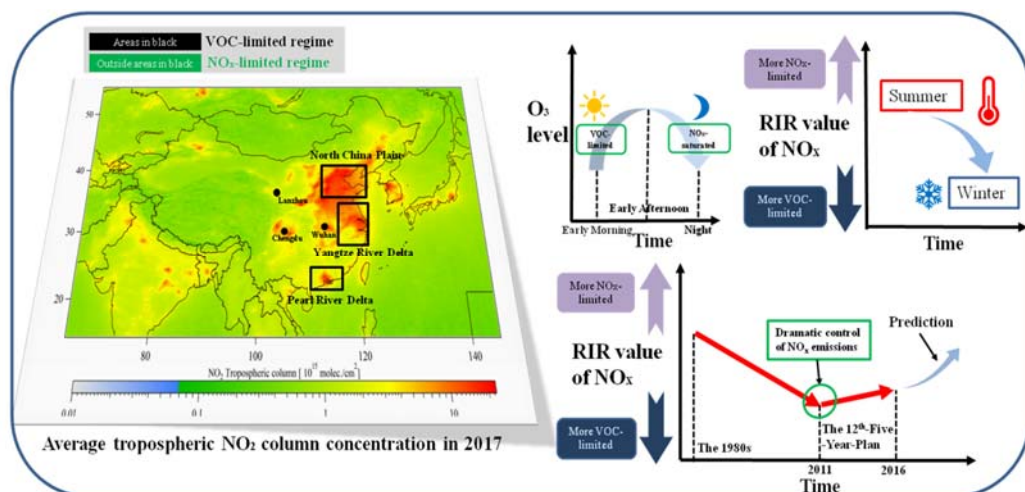
532 Since O<sub>3</sub> is a secondary pollutant, it cannot be controlled directly. Controls of O<sub>3</sub>  
533 pollution should focus on reductions of its precursors. A number of policies were  
534 implemented to control O<sub>3</sub> precursors in recent years. For NO<sub>x</sub>, the emission of NO<sub>x</sub>  
535 from industrial companies and coal-fired power plants had been controlled by the

536 central government since the 12<sup>th</sup> Five-Year-Plan. As for VOCs, [Guo et al. \(2017\)](#)  
537 summarized 23 programs/plans for the control of VOCs in recent years in megacities  
538 (or megacity clusters) in China such as Beijing, Shanghai, Guangdong, Zhejiang and  
539 Jiangsu. The control measures mainly focused on cutting the emissions from vehicles,  
540 vessels and industrial sectors. Although governments have put great efforts on  
541 controlling O<sub>3</sub> pollution (i.e. controls of O<sub>3</sub> precursors), O<sub>3</sub> pollution is still a serious  
542 problem in China and the development of an effective strategy for reducing O<sub>3</sub> pollution  
543 is still problematic due to various characteristics of O<sub>3</sub> pollution (e.g. regionality,  
544 seasonality and severity) and the nonlinear dependency of O<sub>3</sub> formation on NO<sub>x</sub> and  
545 VOCs ([Zhu et al., 2017](#); [Lu et al., 2018](#)). After reviewing and summarizing the spatial-  
546 temporal variations of O<sub>3</sub> formation regimes over China, implications for the control of  
547 O<sub>3</sub> pollution are proposed.

#### 548 **4.1 Precise control of O<sub>3</sub> precursors**

549 In view of the discussions in Sections 2 and 3, precise controls of O<sub>3</sub> precursors are  
550 proposed. On one hand, control measures should vary in different regions/areas  
551 according to the spatial variations of O<sub>3</sub> formation regime. To effectively reduce the O<sub>3</sub>  
552 levels in the three most developed regions (i.e. NCP, YRD and PRD) during the high-  
553 O<sub>3</sub> seasons (summer and autumn), intensive controls of VOCs or both precursors are  
554 effective since most of the areas in these regions are likely VOC-sensitive or mixed-  
555 sensitive due to the vastly anthropogenic emission from populated cities. According to  
556 our previous review on tropospheric VOCs in China ([Guo et al., 2017](#)), the dominant  
557 sources of VOCs emissions in the populated cities of the three regions were summarized.  
558 In brief, vehicular emissions and industrial emissions were the common VOC sources.  
559 In addition, solvent usage made significant contribution to VOCs in PRD. Therefore,  
560 by controlling these sources, VOCs emissions could be effectively reduced in the cities  
561 of the three regions. However, in areas out of these metropolitan cities and/or in the  
562 rural/remote areas in the three regions, O<sub>3</sub> production is mainly limited by NO<sub>x</sub> and thus  
563 reduction of NO<sub>x</sub> emission is more helpful for alleviating O<sub>3</sub> pollution.

564 On the other hand, the priority of control measures should alter with respect to the  
 565 temporal variations of O<sub>3</sub> formation regime. First, although the tremendous emission of  
 566 anthropogenic pollutants leads to the elevated O<sub>3</sub> levels over China, the strong effect of  
 567 NO<sub>x</sub> titration significantly reduces the O<sub>3</sub> levels in populated/urban areas at night.  
 568 However, in rural/remote areas, O<sub>3</sub> may reach the maximum value at dusk and maintain  
 569 a high level at night (Figure 1). Therefore, O<sub>3</sub> pollution at night in rural areas should be  
 570 taken into consideration in term of policy making. Second, enhanced controls of VOCs  
 571 should be adopted in winter since the satellite data showed that O<sub>3</sub> formation regimes  
 572 over China were intended to shift to VOC-limited in winter (Figure 1). Third, due to  
 573 the dramatic emission of NO<sub>x</sub> from traffic and industrial emissions since the 1980s, O<sub>3</sub>  
 574 formation in China moved toward increasing sensitivity to VOC levels. Until the time  
 575 launching the 12<sup>th</sup> Five-Year-Plan, significant controls of NO<sub>x</sub> emission from industry  
 576 successfully reduced the NO<sub>x</sub> levels in China and thus delayed the trend (Figure 1). Due  
 577 to dramatic NO<sub>x</sub> decline in the 12<sup>th</sup> Five-Year-Plan, the effect of NO titration will be  
 578 reduced at night and the minimum level of O<sub>3</sub> may become higher, especially in urban  
 579 areas. Therefore, further intensive control of VOCs is expected in the future to realize  
 580 synchronous reduction of O<sub>3</sub> precursors and eventually achieve O<sub>3</sub> abatement.



581  
 582 Figure 1 Spatial-temporal characteristics of O<sub>3</sub> formation regimes and the implications  
 583 for O<sub>3</sub> pollution control in China  
 584

#### 585 4.2 Joint prevention and control of regional air pollution

586 O<sub>3</sub>, as a secondary pollutant with relatively long lifetime, caused not only an  
587 autochthonous problem but also a regional transboundary problem. O<sub>3</sub> attainment  
588 cannot be simply achieved by the control of pollutant emissions only by local  
589 governments as O<sub>3</sub> and its precursors can transport to the downwind areas with the help  
590 of wind. Also, joint prevention and control of regional air pollution are indispensable  
591 to achieve precise control of O<sub>3</sub> precursors mentioned above. Previous studies pointed  
592 out that regional collaborations were important for developing effective strategies on  
593 air quality improvement and/or sustained O<sub>3</sub> attainment (Jin et al., 2016; Wu et al., 2015;  
594 Wang et al., 2014; Li et al., 2012b). By using the CMAQ model to simulate emission  
595 reduction in BTH and YRD regions, Wang et al. (2014) found that reduction in a  
596 specific province may not only benefit the improvement of local air quality inside the  
597 province, but also has a considerable contribution to the improvement of the air quality  
598 in nearby cities. For example, the 10% emission reduction of SO<sub>2</sub> and NO<sub>x</sub> in Hebei  
599 enhanced the reductions of different pollutants (i.e. NO<sub>2</sub>, SO<sub>4</sub><sup>2-</sup> and NO<sub>3</sub><sup>-</sup>) with 1%~4%  
600 in Beijing and Tianjin. In addition, Xing et al. (2011) examined multiple emission  
601 reduction options using the CMAQ model. It was found that reduction of local NO<sub>x</sub> or  
602 VOC emissions in Beijing was not sufficient to achieve O<sub>3</sub> attainment while  
603 synchronous regional reductions in VOC and NO<sub>x</sub> by 60% to 80% were recommended  
604 across the entire NCP region. Moreover, Wu et al. (2015) proved that joint regional air  
605 pollution control in the BTH region will save the expense on air pollution control  
606 compared to a locally-based pollution control strategy. Taking reduction of SO<sub>2</sub> as an  
607 example, it was estimated that 3.6 billion CNY could be saved if joint regional air  
608 pollution control was implemented in Beijing and its surrounding cities for reducing 6  
609 ppbv of SO<sub>2</sub>. Such strategy is applicable to reductions of other pollutants to save cost  
610 (i.e. NO<sub>x</sub> and VOCs).

611 To effectively proceed regional joint controls, the central government of China has  
612 promulgated a few policies since 2010. For example, nine regions, including the BTH



613 region, the PRD region, the YRD region, central Liaoning region, Shandong Peninsula,  
614 Western Taiwan Straits Metropolitan region, Cheng-Yu Metropolitan region, Wuhan  
615 Metropolitan region, and Cheng-Zhu-Tan region have been designated as the pilot and  
616 key regions by the State Council for the joint prevention and control of regional air  
617 pollutants (i.e. SO<sub>2</sub>, NO<sub>x</sub>, PM and VOCs) in 2010 (Zhou and Elder, 2013). In addition,  
618 the General Office of the State Council published a guideline on strengthening joint  
619 prevention and control of atmospheric pollution to improve air quality on 11 May 2010  
620 ([http://www.gov.cn/gongbao/content/2010/content\\_1612364.htm](http://www.gov.cn/gongbao/content/2010/content_1612364.htm)). In the Guideline,  
621 “joint planning,” “joint monitoring,” “joint supervision,” “joint assessment,” and “joint  
622 coordination” were proposed for regional air pollution management. In particular, a  
623 number of measures were proposed, including 1) implementation of the discharge  
624 permit system; 2) build-up of stronger environmental protection verification systems  
625 for key industries; 3) development of a franchising system for the construction and  
626 operation of pollution control facilities; 4) establishment of stronger environmental  
627 information disclosure system, and 5) development of a system of compliance  
628 management of urban air quality standards.

629 As a matter of fact, several regions/cities followed the guideline and implemented joint  
630 control measures for regional pollution in recent years. For instance, in November 2017,  
631 three cities, including Harbin, Daqing and Suihua, jointly signed a protocol on joint  
632 prevention and control of regional air pollution, in which it required to build  
633 environmental information sharing system, promote prohibition of straw burning and  
634 utilization of straw, and establish coordination mechanism for heavy polluted events  
635 (<http://www.hlj.gov.cn/zwfb/system/2017/11/04/010853072.shtml>). Moreover, to  
636 efficiently improve the regional air quality in Beijing and its surrounding areas, the  
637 Beijing Municipal Environmental Protection Bureau solicited public opinions in March  
638 2014 in regard to the implementation of joint prevention and control of regional air  
639 pollution in six cities, including Beijing, Tianjin, Hebei, Shanxi, Shandong and inner  
640 Mongolia (<http://www.bjepb.gov.cn/bjhrb/hdjl/jyxc/lflkgzjzhzdcsgqzyj/index.html>).

641 In addition to the above nine regions, a new and enhanced network was proposed and  
642 established in September 2014, named Guangdong-Hong Kong-Macao PRD Regional  
643 Air Quality Monitoring Network, aiming to 1) provide accurate data to help three  
644 Governments appraise the air quality in the PRD and formulate appropriate control  
645 measures; 2) evaluate the effectiveness of executed control measures through long-term  
646 monitoring; and 3) provide the detailed information of air quality to the public.

647 Although air pollution seems to be a persistent problem due to the on-going  
648 urbanization and industrialization, it is expected that the air quality would be gradually  
649 improved if there are monitoring stations monitoring air quality and appropriate control  
650 measures are implemented.

651 **Acknowledgement:**

652 This study is supported by the National Key R&D Program of China via grant No.  
653 2017YFC0212001, the Research Grants Council of the Hong Kong Special  
654 Administrative Region Government via grant PolyU 152052/16E and CRF/C5004-15E,  
655 and the Hong Kong PhD Fellowship (Project Number: RULW).

656

657 **References:**

- 658 An, J., Zou, J., Wang, J., Lin, X. & Zhu, B. 2015. Differences in ozone photochemical  
659 characteristics between the megacity Nanjing and its suburban surroundings,  
660 Yangtze River Delta, China. *Environmental Science and Pollution Research*, 22,  
661 19607-19617.
- 662 Aneja, V. P., Brittig, J. S., Kim, D.-S. & Hanna, A. 2004. Ozone and other air quality-  
663 related variables affecting visibility in the Southeast United States. *Journal of the*  
664 *Air & Waste Management Association*, 54, 681-688.
- 665 Altshuller, A. P. 1984. Assessment of the contribution of stratospheric ozone to ground-  
666 level ozone concentrations. *In Assessment of the contribution of stratospheric ozone*  
667 *to ground-level ozone concentrations*. EPA.
- 668 Barker, J. R. 1995. *Progress and problems in atmospheric chemistry* (Vol. 3). World  
669 Scientific.
- 670 Bhatia, A., Tomer, R., Kumar, V., Singh, S. & Pathak, D. S. 2012. *Impact of*  
671 *tropospheric ozone on crop growth and productivity-a review*.
- 672 Brown, S. S. & Stutz, J. 2012. Nighttime radical observations and chemistry. *Chemical*  
673 *Society Reviews*, 41, 6405-6447.
- 674 Cheng, H., Guo, H., Wang, X., Saunders, S. M., Lam, S., Jiang, F., Wang, T., Ding, A.,

675 Lee, S. & Ho, K. 2010. On the relationship between ozone and its precursors in the  
676 Pearl River Delta: application of an observation-based model (OBM).  
677 *Environmental Science and Pollution Research*, 17, 547-560.

678 Chou, C. C.-K., Tsai, C.-Y., Shiu, C.-J., Liu, S. C. & Zhu, T. 2009. Measurement of  
679 NO<sub>y</sub> during Campaign of Air Quality Research in Beijing 2006 (CAREBeijing-  
680 2006): Implications for the ozone production efficiency of NO<sub>x</sub>. *Journal of*  
681 *Geophysical Research: Atmospheres*, 114.

682 Diao, B., Ding, L., Su, P. & Cheng, J. 2018. The spatial-temporal characteristics and  
683 influential factors of NO<sub>x</sub> emissions in China: A spatial econometric analysis.  
684 *International journal of environmental research and public health*, 15, 1405.

685 Ding, A., Fu, C., Yang, X., Sun, J., Zheng, L., Xie, Y., Herrmann, E., Nie, W., Petäjä, T.  
686 & Kerminen, V.-M. 2013. Ozone and fine particle in the western Yangtze River Delta:  
687 an overview of 1 yr data at the SORPES station. *Atmospheric Chemistry and Physics*,  
688 13, 5813-5830.

689 Geng, F., Tie, X., Xu, J., Zhou, G., Peng, L., Gao, W., Tang, X. & Zhao, C. 2008.  
690 Characterizations of ozone, NO<sub>x</sub>, and VOCs measured in Shanghai, China.  
691 *Atmospheric Environment*, 42, 6873-6883.

692 Guo, H., Jiang, F., Cheng, H., Simpson, I., Wang, X., Ding, A., Wang, T., Saunders, S.,  
693 Wang, T. & Lam, S. 2009. Concurrent observations of air pollutants at two sites in  
694 the Pearl River Delta and the implication of regional transport. *Atmospheric*  
695 *Chemistry and Physics*, 9, 7343-7360.

696 Guo, H., Ling, Z., Cheng, H., Simpson, I., Lyu, X., Wang, X., Shao, M., Lu, H., Ayoko,  
697 G. & Zhang, Y. 2017. Tropospheric volatile organic compounds in China. *Science of*  
698 *the Total Environment*, 574, 1021-1043.

699 Guo, H., Ling, Z., Cheung, K., Jiang, F., Wang, D., Simpson, I., Barletta, B., Meinardi,  
700 S., Wang, T. & Wang, X. 2013. Characterization of photochemical pollution at  
701 different elevations in mountainous areas in Hong Kong. *Atmospheric Chemistry*  
702 *and Physics*, 13, 3881-3898.

703 Goodman, J. E., Prueitt, R. L., Sax, S. N., Pizzurro, D. M., Lynch, H. N., Zu, K. &  
704 Venditti, F. J. 2015. Ozone exposure and systemic biomarkers: Evaluation of  
705 evidence for adverse cardiovascular health impacts. *Critical Reviews in Toxicology*,  
706 45, 412-452.

707 Han, S., Zhang, M., Zhao, C., Lu, X., Ran, L., Han, M., Li, P.-Y. & Li, X.-J. 2013.  
708 Differences in ozone photochemical characteristics between the megacity Tianjin  
709 and its rural surroundings. *Atmospheric environment*, 79, 209-216.

710 Han, X., Zhu, L., Wang, S., Meng, X., Zhang, M. & Hu, J. 2018. Modeling study of  
711 impacts on surface ozone of regional transport and emission reductions over North  
712 China Plain in summer 2015. *Atmospheric Chemistry and Physics Discussions*, 1-  
713 32.

714 He, J., Wang, Y., Hao, J., Shen, L. & Wang, L. 2012. Variations of surface O<sub>3</sub> in August  
715 at a rural site near Shanghai: influences from the West Pacific subtropical high and  
716 anthropogenic emissions. *Environmental Science and Pollution Research*, 19, 4016-

717 4029.

718 Huang, J. P., Fung, J. C., Lau, A. K. & Qin, Y. 2005. Numerical simulation and process  
719 analysis of typhoon-related ozone episodes in Hong Kong. *Journal of Geophysical*  
720 *Research: Atmospheres*, 110.

721 Jenkin, M. E. & Clemitshaw, K. C. 2000. Ozone and other secondary photochemical  
722 pollutants: chemical processes governing their formation in the planetary boundary  
723 layer. *Atmospheric Environment*, 34, 2499-2527.

724 Jia, C., Mao, X., Huang, T., Liang, X., Wang, Y., Shen, Y., Jiang, W., Wang, H., Bai, Z.  
725 & Ma, M. 2016. Non-methane hydrocarbons (NMHCs) and their contribution to  
726 ozone formation potential in a petrochemical industrialized city, Northwest China.  
727 *Atmospheric Research*, 169, 225-236.

728 Jin, X. & Holloway, T. 2015. Spatial and temporal variability of ozone sensitivity over  
729 China observed from the Ozone Monitoring Instrument. *Journal of Geophysical*  
730 *Research: Atmospheres*, 120, 7229-7246.

731 Jin, Y., Andersson, H. & Zhang, S. 2016. Air pollution control policies in China: A  
732 retrospective and prospects. *International journal of environmental research and*  
733 *public health*, 13, 1219.

734 Lam, S., Saunders, S., Guo, H., Ling, Z., Jiang, F., Wang, X. & Wang, T. 2013.  
735 Modelling VOC source impacts on high ozone episode days observed at a mountain  
736 summit in Hong Kong under the influence of mountain-valley breezes. *Atmospheric*  
737 *environment*, 81, 166-176.

738 Li, L., Chen, C., Huang, C., Huang, H., Zhang, G., Wang, Y., Wang, H., Lou, S., Qiao,  
739 L. & Zhou, M. 2012a. Process analysis of regional ozone formation over the Yangtze  
740 River Delta, China using the Community Multi-scale Air Quality modeling system.  
741 *Atmospheric Chemistry and Physics*, 12, 10971-10987.

742 Li, Y., Lau, A. K.-H., Fung, J. C.-H., Zheng, J., Zhong, L. & Louie, P. K. K. 2012b.  
743 Ozone source apportionment (OSAT) to differentiate local regional and super-  
744 regional source contributions in the Pearl River Delta region, China. *Journal of*  
745 *Geophysical Research: Atmospheres*, 117.

746 Li, K., Jacob, D. J., Liao, H., Shen, L., Zhang, Q., & Bates, K. H. 2019. Anthropogenic  
747 drivers of 2013–2017 trends in summer surface ozone in China. *Proceedings of the*  
748 *National Academy of Sciences*, 116(2), 422-427.

749 Lin, W., Xu, X., Ge, B. & Zhang, X. 2009. Characteristics of gaseous pollutants at  
750 Gucheng, a rural site southwest of Beijing. *Journal of Geophysical Research:*  
751 *Atmospheres*, 114.

752 Ling, Z. & Guo, H. 2014. Contribution of VOC sources to photochemical ozone  
753 formation and its control policy implication in Hong Kong. *Environmental science*  
754 *& policy*, 38, 180-191.

755 Liu, B., Liang, D., Yang, J., Dai, Q., Bi, X., Feng, Y., Yuan, J., Xiao, Z., Zhang, Y. &  
756 Xu, H. 2016. Characterization and source apportionment of volatile organic  
757 compounds based on 1-year of observational data in Tianjin, China. *Environmental*  
758 *pollution*, 218, 757-769.

759 Liu, X., Zhang, Y., Cheng, S., Xing, J., Zhang, Q., Streets, D. G., Jang, C., Wang, W. &  
760 Hao, J. 2010. Understanding of regional air pollution over China using CMAQ, part  
761 I performance evaluation and seasonal variation. *Atmospheric Environment*, 44,  
762 2415-2426.

763 Liu, Z., Wang, Y., Gu, D., Zhao, C., Huey, L., Stickel, R., Liao, J., Shao, M., Zhu, T. &  
764 Zeng, L. 2012. Summertime photochemistry during CAREBeijing-2007: RO<sub>x</sub>  
765 budgets and O<sub>3</sub> formation. *Atmospheric Chemistry and Physics*, 12, 7737-7752.

766 Lu, K., Zhang, Y., Su, H., Brauers, T., Chou, C. C., Hofzumahaus, A., Liu, S. C., Kita,  
767 K., Kondo, Y. & Shao, M. 2010. Oxidant (O<sub>3</sub>+ NO<sub>2</sub>) production processes and  
768 formation regimes in Beijing. *Journal of Geophysical Research: Atmospheres*, 115.

769 Lu, X., Hong, J., Zhang, L., Cooper, O. R., Schultz, M. G., Xu, X., Wang, T., Gao, M.,  
770 Zhao, Y. & Zhang, Y. 2018. Severe surface ozone pollution in China: A global  
771 perspective. *Environmental Science & Technology Letters*, 5(8), 487-494.

772 Lyu, X., Chen, N., Guo, H., Zhang, W., Wang, N., Wang, Y. & Liu, M. 2016. Ambient  
773 volatile organic compounds and their effect on ozone production in Wuhan, central  
774 China. *Science of the total environment*, 541, 200-209.

775 Ma, Z., Wang, Y., Zhang, X. & Xu, J. 2011. Comparison of ozone between Beijing and  
776 downstream area. *Huanjing Kexue = Chinese Journal of Environmental Science*, 32,  
777 924-929.

778 Ma, Z., Xu, J., Quan, W., Zhang, Z., Lin, W. & Xu, X. 2016. Significant increase of  
779 surface ozone at a rural site, north of eastern China. *Atmospheric Chemistry and  
780 Physics*, 16, 3969-3977.

781 Ogundele, F. O., Omotayo, A. & Taiwo, I. 2011. The dilemma of ozone layer depletion,  
782 global warming and climate change in tropical countries: A review. *Academic  
783 Research International*, 1, 474.

784 Ou, J., Yuan, Z., Zheng, J., Huang, Z., Shao, M., Li, Z., Huang, X., Guo, H. & Louie,  
785 P. K. 2016. Ambient ozone control in a photochemically active region: short-term  
786 despiking or long-term attainment? *Environmental science & technology*, 50, 5720-  
787 5728.

788 Pusede, S. E., Steiner, A. L., & Cohen, R. C. 2015. Temperature and recent trends in  
789 the chemistry of continental surface ozone. *Chemical reviews*, 115(10), 3898-3918.

790 Ran, L., Zhao, C., Geng, F., Tie, X., Tang, X., Peng, L., Zhou, G., Yu, Q., Xu, J. &  
791 Guenther, A. 2009. Ozone photochemical production in urban Shanghai, China:  
792 Analysis based on ground level observations. *Journal of Geophysical Research:  
793 Atmospheres*, 114.

794 Ran, L., Zhao, C., Xu, W., Lu, X., Han, M., Lin, W., Yan, P., Xu, X., Deng, Z. & Ma,  
795 N. 2011. VOC reactivity and its effect on ozone production during the HaChi  
796 summer campaign. *Atmospheric Chemistry and Physics*, 11, 4657-4667.

797 Reddy, B. S. K., Reddy, L. S. S., Cao, J. J., Kumar, K. R., Balakrishnaiah, G., Gopal,  
798 K. R., Reddy, R. R., Narasimhulu, K., LaI, S. & Ahammed, Y. N. 2011. Simultaneous  
799 measurements of surface ozone at two sites over the Southern Asia: a comparative  
800 study. *Aerosol and Air Quality Research*, 11(7), 895-902.

- 801 Russell, A., & Dennis, R. 2000. NARSTO critical review of photochemical models and  
802 modeling. *Atmospheric environment*, 34(12-14), 2283-2324.
- 803 Shao, M., Lu, S., Liu, Y., Xie, X., Chang, C., Huang, S. & Chen, Z. 2009a. Volatile  
804 organic compounds measured in summer in Beijing and their role in ground-level  
805 ozone formation. *Journal of Geophysical Research: Atmospheres*, 114.
- 806 Shao, M., Zhang, Y., Zeng, L., Tang, X., Zhang, J., Zhong, L. & Wang, B. 2009b.  
807 Ground-level ozone in the Pearl River Delta and the roles of VOC and NO<sub>x</sub> in its  
808 production. *Journal of Environmental Management*, 90, 512-518.
- 809 Sillman, S. 1995. The use of NO<sub>y</sub>, H<sub>2</sub>O<sub>2</sub>, and HNO<sub>3</sub> as indicators for ozone-NO<sub>x</sub>-  
810 hydrocarbon sensitivity in urban locations. *Journal of Geophysical Research:*  
811 *Atmospheres*, 100, 14175-14188.
- 812 Sillman, S. 1999. The relation between ozone, NO<sub>x</sub> and hydrocarbons in urban and  
813 polluted rural environments. *Atmospheric Environment*, 33, 1821-1845.
- 814 Sousa, S. I., Alvim-Ferraz, M. C. & Martins, F. G. 2013. Health effects of ozone  
815 focusing on childhood asthma: what is now known--a review from an  
816 epidemiological point of view. *Chemosphere*, 90, 2051-8.
- 817 Steinfeld, J. I. 1998. Atmospheric chemistry and physics: from air pollution to climate  
818 change. *Environment: Science and Policy for Sustainable Development*, 40, 26-26.
- 819 Tan, Z., Lu, K., Jiang, M., Su, R., Dong, H., Zeng, L., Xie, S., Tan, Q. & Zhang, Y.  
820 2018. Exploring ozone pollution in Chengdu, southwestern China: A case study from  
821 radical chemistry to O<sub>3</sub>-VOC-NO<sub>x</sub> sensitivity. *Science of The Total Environment*,  
822 636, 775-786.
- 823 Tang, W., Zhao, C., Geng, F., Peng, L., Zhou, G., Gao, W., Xu, J. & Tie, X. 2008. Study  
824 of ozone “weekend effect” in Shanghai. *Science in China Series D: Earth Sciences*,  
825 51, 1354-1360.
- 826 Tang, X., Wang, Z., Zhu, J., Gbaguidi, A. E., Wu, Q., Li, J. & Zhu, T. 2010. Sensitivity  
827 of ozone to precursor emissions in urban Beijing with a Monte Carlo scheme.  
828 *Atmospheric Environment*, 44, 3833-3842.
- 829 Tonnesen, G. S. & Dennis, R. L. 2000. Analysis of radical propagation efficiency to  
830 assess ozone sensitivity to hydrocarbons and NO<sub>x</sub>: 1. Local indicators of  
831 instantaneous odd oxygen production sensitivity. *Journal of Geophysical Research:*  
832 *Atmospheres*, 105, 9213-9225.
- 833 Tu, J., Xia, Z., Wang, H. & Li, W. 2007. Temporal variations in surface ozone and its  
834 precursors and meteorological effects at an urban site in China. *Atmospheric*  
835 *Research*, 85, 310-337.
- 836 Wang, T., Ding, A., Gao, J. & Wu, W. S. 2006a. Strong ozone production in urban  
837 plumes from Beijing, China. *Geophysical Research Letters*, 33.
- 838 Wang, H., Zhou, L. & Tang, X. 2006b. Ozone concentrations in rural regions of the  
839 Yangtze Delta in China. *Journal of Atmospheric chemistry*, 54, 255-265.
- 840 Wang, S., Xing, J., Zhao, B., Jang, C. & Hao, J. 2014. Effectiveness of national air  
841 pollution control policies on the air quality in metropolitan areas of China. *Journal*  
842 *of Environmental Sciences*, 26, 13-22.

- 843 Wang, T., Wei, X., Ding, A., Poon, S. C., Lam, K., Li, Y., Chan, L. & Anson, M. 2009.  
844 Increasing surface ozone concentrations in the background atmosphere of Southern  
845 China, 1994-2007. *Atmospheric Chemistry and Physics*.
- 846 Wang, T., Xue, L., Brimblecombe, P., Lam, Y. F., Li, L. & Zhang, L. 2017a. Ozone  
847 pollution in China: A review of concentrations, meteorological influences, chemical  
848 precursors, and effects. *Science of the Total Environment*, 575, 1582-1596.
- 849 Wang, W., Cheng, T., Gu, X., Chen, H., Guo, H., Wang, Y., Bao, F., Shi, S., Xu, B. &  
850 Zuo, X. 2017b. Assessing spatial and temporal patterns of observed ground-level  
851 ozone in China. *Scientific Reports*, 7, 3651.
- 852 Wang, X., Zhang, Y., Hu, Y., Zhou, W., Lu, K., Zhong, L., Zeng, L., Shao, M., Hu, M.  
853 & Russell, A. 2010. Process analysis and sensitivity study of regional ozone  
854 formation over the Pearl River Delta, China, during the PRIDE-PRD2004 campaign  
855 using the Community Multiscale Air Quality modeling system. *Atmospheric  
856 Chemistry and Physics*, 10, 4423-4437.
- 857 Wang, Y., Guo, H., Zou, S., Lyu, X., Ling, Z., Cheng, H. & Zeren, Y. 2018. Surface O<sub>3</sub>  
858 photochemistry over the South China Sea: Application of a near-explicit chemical  
859 mechanism box model. *Environmental Pollution*, 234, 155-166.
- 860 Wei, W., Cheng, S., Wang, L., Ji, D., Zhou, Y., Han, L. & Wang, L. 2015. Characterizing  
861 ozone pollution in a petrochemical industrial area in Beijing, China: a case study  
862 using a chemical reaction model. *Environmental monitoring and assessment*, 187,  
863 377.
- 864 Wu, D., Xu, Y. & Zhang, S. 2015. Will joint regional air pollution control be more cost-  
865 effective? An empirical study of China's Beijing-Tianjin-Hebei region. *Journal of  
866 environmental management*, 149, 27-36.
- 867 Wu, R. & Xie, S. 2017. Spatial distribution of ozone formation in China derived from  
868 emissions of speciated volatile organic compounds. *Environmental science &  
869 technology*, 51, 2574-2583.
- 870 Wu, W., Xue, W., Lei, Y. & Wang, J. 2018. Sensitivity analysis of ozone in Beijing-  
871 Tianjin-Hebei (BTH) and its surrounding area using OMI satellite remote sensing  
872 data. *CHINA ENVIRONMENTAL SCIENCECE*, 38, 1201-1208.
- 873 Xing, J., Wang, S., Jang, C., ZHU, Y. & HAO, J. 2011. Nonlinear response of ozone to  
874 precursor emission changes in China: a modeling study using response surface  
875 methodology. *Atmospheric Chemistry and Physics*, 11, 5027-5044.
- 876 Xu, J., Zhang, X., Xu, X., Zhao, X., Meng, W. & Pu, W. 2011. Measurement of surface  
877 ozone and its precursors in urban and rural sites in Beijing. *Procedia Earth and  
878 Planetary Science*, 2, 255-261.
- 879 Xu, J., Zhang, Y., Fu, J. S., Zheng, S. & Wang, W. 2008. Process analysis of typical  
880 summertime ozone episodes over the Beijing area. *Science of the Total Environment*,  
881 399, 147-157.
- 882 Xu, X., Lin, W., Wang, T., Yan, P., Tang, J., Meng, Z., & Wang, Y. 2008. Long-term  
883 trend of surface ozone at a regional background station in eastern China 1991–2006:  
884 enhanced variability. *Atmospheric Chemistry and Physics*, 8(10), 2595-2607.

885 Xu, Z., Huang, X., Nie, W., Chi, X., Xu, Z., Zheng, L., Sun, P. & Ding, A. 2017.  
886 Influence of synoptic condition and holiday effects on VOCs and ozone production  
887 in the Yangtze River Delta region, China. *Atmospheric Environment*, 168, 112-124.  
888 Xue, L., Wang, T., Gao, J., Ding, A., Zhou, X., Blake, D., Wang, X., Saunders, S., Fan,  
889 S. & Zuo, H. 2014. Ground-level ozone in four Chinese cities: precursors, regional  
890 transport and heterogeneous processes. *Atmospheric Chemistry and Physics*, 14,  
891 13175-13188.  
892 Zhang, Q., Yuan, B., Shao, M., Wang, X., Lu, S., Lu, K., Wang, M., Chen, L., Chang,  
893 C.-C. & Liu, S. 2014. Variations of ground-level O<sub>3</sub> and its precursors in Beijing in  
894 summertime between 2005 and 2011. *Atmospheric Chemistry and Physics*, 14, 6089-  
895 6101.  
896 Zhang, Y., Su, H., Zhong, L., Cheng, Y., Zeng, L., Wang, X., Xiang, Y., Wang, J., Gao,  
897 D. & Shao, M. 2008. Regional ozone pollution and observation-based approach for  
898 analyzing ozone-precursor relationship during the PRIDE-PRD2004 campaign.  
899 *Atmospheric Environment*, 42, 6203-6218.  
900 Zhang, Y., Vijayaraghavan, K., Wen, X., Snell, H. & Jacobson, M. 2009. Probing into  
901 regional O<sub>3</sub> and PM pollution in the US, Part I. A 1-year CMAQ simulation and  
902 evaluation using surface and satellite data. *Journal of Geophysical Research*, 114.  
903 Zheng, J., Zhong, L., Wang, T., Louie, P. K. & Li, Z. 2010. Ground-level ozone in the  
904 Pearl River Delta region: analysis of data from a recently established regional air  
905 quality monitoring network. *Atmospheric Environment*, 44, 814-823.  
906 Zhou, X. & Elder, M. 2013. Regional air quality management in China: the 2010  
907 guideline on strengthening joint prevention and control of atmospheric pollution.  
908 *International Journal of Sustainable Society*, 5, 232-249.  
909 Zhu, C., Zhang, N. & Shi, Y. 2017. Consideration on Features of Ozone Pollution and  
910 Countermeasure. *Huanjingbaohu*, 16, 64-66.  
911 Zong, R., Yang, X., Wen, L., Xu, C., Zhu, Y., Chen, T., Yao, L., Wang, L., Zhang, J. &  
912 Yang, L. 2018. Strong ozone production at a rural site in the North China Plain:  
913 Mixed effects of urban plumes and biogenic emissions. *Journal of Environmental*  
914 *Sciences*.  
915 Zou, Y., Deng, X., Zhu, D., Gong, D., Wang, H., Li, F., Tan, H., Deng, T., Mai, B. &  
916 Liu, X. 2015. Characteristics of 1 year of observational data of VOCs, NO<sub>x</sub> and O<sub>3</sub>  
917 at a suburban site in Guangzhou, China. *Atmospheric Chemistry and Physics*, 15,  
918 6625-6636.  
919